

Electronic Supplementary Information

Amide-induced phase separation of hexafluoroisopropanol–water mixtures depending on the hydrophobicity of amide

Toshiyuki Takamuku,^{*a} Hiroshi Wada,^a Chiemi Kawatoko,^a Takuya Shimomura,^a Ryo Kanzaki^b and Munetaka Takeuchi^c

^a *Department of Chemistry and Applied Chemistry, Graduate School of Science and Engineering, Saga University, Honjo-machi, Saga 840-8502, Japan; E-mail: takamut@cc.saga-u.ac.jp.*

^b *Graduate School of Science and Engineering, Kagoshima University, Korimoto, Kagoshima 890-0065, Japan*

^c *Fujitsu Limited, Nakase 1-chome, Mihama-ku, Chiba 269-8588, Japan*

Table S1 Compositions of amide–HFIP–D₂O mixtures for SANS measurements and their Ornstein–Zernike correlation lengths ξ determined by SANS measurements at 298 K.^a

Sample	x_A	x_{HFIP}	x_{Water}	x_{HFIP}^S	$x_A/x_{A,298}^L$	$x_A/x_{A,298}^U$	$\xi/\text{\AA}$
NMF							
F0 _S	0	0.147	0.853	0.147	0		4.8(1)
F1 _S	0.00770	0.146	0.846	0.147	35		6.8(1)
F2 _S	0.0132	0.145	0.842	0.147	60		9.4(1)
F3 _S	0.0175	0.145	0.838	0.147	80		12.2(1)
F4 _S	0.0198	0.144	0.836	0.147	90		15.1(1)
F5 _S	0.199	0.118	0.683	0.147		103	29.2(1)
F6 _S	0.204	0.117	0.679	0.147		106	22.7(1)
F7 _S	0.212	0.116	0.672	0.147		110	17.3(1)
F8 _S	0.222	0.115	0.663	0.147		115	14.1(1)
F9 _S	0.232	0.113	0.655	0.147		120	11.8(1)
NMA							
A0 _S	0	0.147	0.853	0.147	0		4.8(1)
A1 _S	0.00520	0.147	0.848	0.147	35		7.0(1)
A2 _S	0.00900	0.146	0.845	0.147	60		9.8(1)
A3 _S	0.0120	0.146	0.843	0.147	80		13.6(1)
A4 _S	0.0135	0.145	0.841	0.147	90		16.8(1)
A5 _S	0.248	0.111	0.641	0.147		103	29.8(1)
A6 _S	0.256	0.110	0.635	0.147		107	21.3(1)
A7 _S	0.265	0.108	0.627	0.147		110	17.1(1)
A8 _S	0.277	0.107	0.617	0.147		115	13.4(1)
A9 _S	0.289	0.105	0.606	0.147		120	
NMP							
P0 _S	0	0.147	0.853	0.147	0		4.8(1)
P1 _S	0.00440	0.147	0.849	0.147	35		7.3(1)
P2 _S	0.00750	0.146	0.846	0.147	60		10.1(1)
P3 _S	0.0100	0.146	0.844	0.147	80		12.7(1)
P4 _S	0.0113	0.146	0.843	0.147	90		18.2(1)
P5 _S	0.294	0.104	0.602	0.147		103	19.1(1)
P6 _S	0.303	0.103	0.594	0.147		106	13.3(1)
P7 _S	0.315	0.101	0.584	0.147		110	12.2(1)
P8 _S	0.328	0.0989	0.573	0.147		115	10.6(1)
P9 _S	0.343	0.0967	0.560	0.147		120	

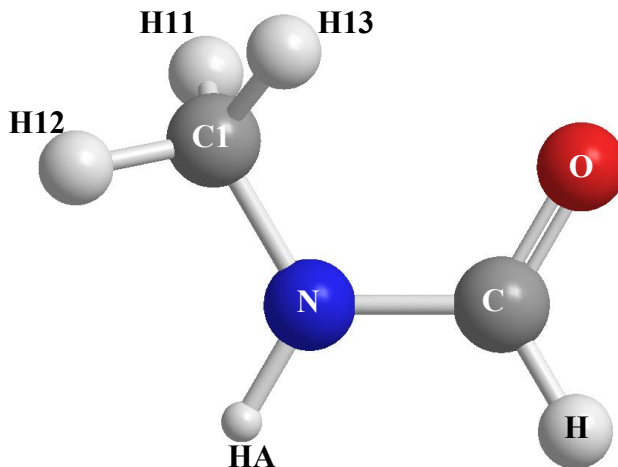
^a x_{HFIP}^S gives the HFIP mole fractions of HFIP–water binary solvent. $x_A/x_{A,298}^L$ and $x_A/x_{A,298}^U$ represent the ratios of amide mole fraction to the lower and upper phase separation mole fractions, respectively, in percent figures. The phase separation mole fractions $x_{A,298}^L$ and $x_{A,298}^U$ are listed in Table 2. The values in the parentheses are standard deviations.

Table S2 Compositions of amide–HFIP–H₂O mixtures for NMR measurements.

Sample	x_A	x_{HFIP}	x_{Water}	x_{HFIP}^S	$x_A/x_{A,298}^L$	$x_A/x_{A,298}^U$
NMF						
F1 _N	0.00832	0.146	0.846	0.147	34	
F2 _N	0.0139	0.145	0.841	0.147	57	
F3 _N	0.0210	0.144	0.835	0.147	87	
F4 _N	0.0235	0.144	0.833	0.147	97	
F5 _N	0.195	0.118	0.687	0.147		103
F6 _N	0.197	0.118	0.685	0.147		104
F7 _N	0.207	0.117	0.676	0.147		110
F8 _N	0.218	0.115	0.667	0.147		115
F9 _N	0.237	0.112	0.651	0.147		125
NMA						
A1 _N	0.00550	0.146	0.848	0.147	34	
A2 _N	0.00902	0.146	0.845	0.147	55	
A3 _N	0.0136	0.145	0.841	0.147	83	
A4 _N	0.0155	0.145	0.840	0.147	95	
A5 _N	0.252	0.110	0.638	0.147		105
A6 _N	0.257	0.109	0.634	0.147		107
A7 _N	0.266	0.108	0.626	0.147		111
A8 _N	0.278	0.106	0.616	0.147		116
A9 _N	0.302	0.103	0.595	0.147		126
NMP						
P1 _N	0.00388	0.146	0.850	0.147	28	
P2 _N	0.00657	0.146	0.847	0.147	54	
P3 _N	0.00972	0.146	0.845	0.147	80	
P4 _N	0.0111	0.145	0.844	0.147	91	
P5 _N	0.298	0.103	0.599	0.147		105
P6 _N	0.303	0.102	0.594	0.147		106
P7 _N	0.309	0.102	0.590	0.147		108
P8 _N	0.324	0.0993	0.576	0.147		114
P9 _N	0.357	0.0946	0.549	0.147		125

Table S3 Intramolecular atom–atom bond lengths and notation of the atoms in NMF, NMA, and NMP and the potential parameters used for the MD simulations.

Intramolecular Atom–Atom Bond Lengths		
Molecule	Bond	$r / \text{Å}$
NMF	C1–H11	1.090
	C1–H12	1.090
	C1–H13	1.090
	C1–N	1.449
	HA–N	1.010
	C–N	1.335
	C–H	1.080
	C–O	1.229



Bond Angle Potentials			
Molecule	Angle	$K_\theta / \text{kcal mol}^{-1} \text{ rad}^{-2}$	θ_0 / deg
NMF	H11–C1–H12	35	109.5
	H11–C1–H13	35	109.5
	H12–C1–H13	35	109.5
	H11–C1–N	38	109.5
	H12–C1–N	38	109.5
	H13–C1–N	38	109.5
	C1–N–HA	38	118.4
	C1–N–C	50	121.9
	HA–N–C	35	119.8
	N–C–O	80	122.9
	N–C–H	35	119.1
	H–C–O	80	122.9

(Cont.)

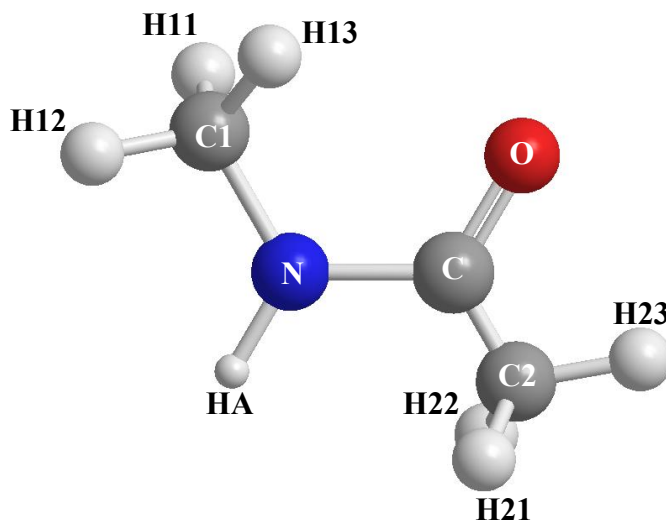
Torsion Potentials				
Molecule	Torsion	$V_n/2 / \text{kcal mol}^{-1}$	n	ϕ_0 / deg
NMF	H11-C1-N-HA	0	3	0
	H12-C1-N-HA	0	3	0
	H13-C1-N-HA	0	3	0
	H11-C1-N-C	0	3	0
	H12-C1-N-C	0	3	0
	H13-C1-N-C	0	3	0
	C1-N-C-O	10	2	180
	HA-N-C-O	10	2	180
	C1-N-C-H	10	2	180
	HA-N-C-H	10	2	180

van der Waals Parameters and Point Charges				
Molecule	Atom	$\sigma / \text{Å}$	$\epsilon / \text{kcal mol}^{-1}$	q / e
NMF	C1	3.500	0.066	0.020
	HA	0.000	0.000	0.300
	N	3.250	0.170	-0.500
	C	3.750	0.105	0.500
	O	2.960	0.210	-0.500
	H11	2.500	0.030	0.060
	H12	2.500	0.030	0.060
	H13	2.500	0.030	0.060
	H	2.420	0.015	0.000

(Cont.)

Intramolecular Atom–Atom Bond Lengths

Molecule	Bond	$r / \text{Å}$
NMA	C1–H11	1.090
	C1–H12	1.090
	C1–H13	1.090
	C1–N	1.449
	HA–N	1.010
	C–N	1.335
	C–O	1.229
	C–C2	1.522
	C2–H21	1.090
	C2–H22	1.090
	C2–H23	1.090



Bond Angle Potentials

Molecule	Angle	$K_0 / \text{kcal mol}^{-1} \text{rad}^{-2}$	θ_0 / deg
NMA	H11–C1–H12	35	109.5
	H11–C1–H13	35	109.5
	H12–C1–H13	35	109.5
	H11–C1–N	38	109.5
	H12–C1–N	38	109.5
	H13–C1–N	38	109.5
	C1–N–HA	38	118.4
	C1–N–C	50	121.9
	HA–N–C	35	119.8
	N–C–O	80	122.9
	N–C–C2	70	116.6

(Cont.)

C-C2-H21	35	109.5
C-C2-H22	35	109.5
C-C2-H23	35	109.5
H21-C2-H22	35	109.5
H21-C2-H23	35	109.5
H22-C2-H23	35	109.5
C2-C-O	87	120.4

Torsion Potentials

Molecule	Torsion	$V_n/2$ / kcal mol ⁻¹	n	ϕ_0 / deg
NMA	H11-C1-N-HA	0	3	0
	H12-C1-N-HA	0	3	0
	H13-C1-N-HA	0	3	0
	H11-C1-N-C	0	3	0
	H12-C1-N-C	0	3	0
	H13-C1-N-C	0	3	0
	C1-N-C-O	10	2	180
	HA-N-C-O	10	2	180
	C1-N-C-C2	10	2	180
	HA-N-C-C2	10	2	180
	N-C-C2-H21	0	2	0
	N-C-C2-H22	0	2	0
	N-C-C2-H23	0	2	0
	O-C-C2-H21	0	2	0
	O-C-C2-H22	0	2	0
	O-C-C2-H23	0	2	0

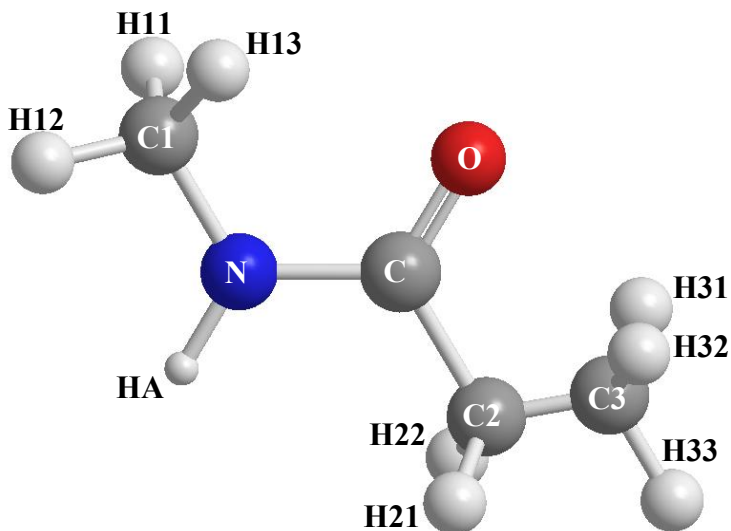
(Cont.)

van der Waals Parameters and Point Charges				
Molecule	Atom	$\sigma / \text{\AA}$	$\varepsilon / \text{kcal mol}^{-1}$	q / e
NMA	C1	3.500	0.066	0.020
	C2	3.500	0.066	-0.180
	HA	0.000	0.000	0.300
	N	3.250	0.170	-0.500
	C	3.750	0.105	0.500
	O	2.960	0.210	-0.500
	H11	2.500	0.030	0.060
	H12	2.500	0.030	0.060
	H13	2.500	0.030	0.060
	H21	2.500	0.030	0.060
	H22	2.500	0.030	0.060
	H23	2.500	0.030	0.060

(Cont.)

Intramolecular Atom–Atom Bond Lengths

Molecule	Bond	$r / \text{Å}$
NMP	C1–H11	1.090
	C1–H12	1.090
	C1–H13	1.090
	C1–N	1.449
	HA–N	1.010
	C–N	1.335
	C–O	1.229
	C–C2	1.522
	C2–C3	1.526
	C2–H21	1.090
	C2–H22	1.090
	C3–H31	1.090
	C3–H32	1.090
	C3–H33	1.090



Bond Angle Potentials

Molecule	Angle	$K_0 / \text{kcal mol}^{-1} \text{rad}^{-2}$	θ_0 / deg
NMP	H11–C1–H12	35	109.5
	H11–C1–H13	35	109.5
	H12–C1–H13	35	109.5
	H11–C1–N	38	109.5
	H12–C1–N	38	109.5
	H13–C1–N	38	109.5
	C1–N–HA	38	118.4
	C1–N–C	50	121.9
	HA–N–C	35	119.8

(Cont.)

N-C-O	80	122.9
N-C-C2	70	116.6
C-C2-H21	35	109.5
C-C2-H22	35	109.5
C-C2-C3	63	111.1
H21-C2-C3	35	109.5
H22-C2-C3	35	109.5
H21-C2-H22	35	109.5
C2-C3-H31	35	109.5
C2-C3-H32	35	109.5
C2-C3-H33	35	109.5
H31-C3-H32	35	109.5
H31-C3-H33	35	109.5
H32-C3-H33	35	109.5
C2-C-O	87	120.4

Torsion Potentials

Molecule	Torsion	$V_n/2 / \text{kcal mol}^{-1}$	n	ϕ_0 / deg
NMP	H11-C1-N-HA	0	3	0
	H12-C1-N-HA	0	3	0
	H13-C1-N-HA	0	3	0
	H11-C1-N-C	0	3	0
	H12-C1-N-C	0	3	0
	H13-C1-N-C	0	3	0
	C1-N-C-O	10	2	180
	HA-N-C-O	10	2	180
	C1-N-C-C2	10	2	180
	HA-N-C-C2	10	2	180

(Cont.)

N-C-C2-C3	0	2	0
N-C-C2-H21	0	2	0
N-C-C2-H22	0	2	0
O-C-C2-H21	0	2	0
O-C-C2-H22	0	2	0
O-C-C2-C3	0	2	0
H21-C2-C3-H31	1.3	3	0
H21-C2-C3-H32	1.3	3	0
H21-C2-C3-H33	1.3	3	0
H22-C2-C3-H31	1.3	3	0
H22-C2-C3-H32	1.3	3	0
H22-C2-C3-H33	1.3	3	0
C-C2-C3-H31	1.3	3	0
C-C2-C3-H32	1.3	3	0
C-C2-C3-H33	1.3	3	0

van der Waals Parameters and Point Charges

Molecule	Atom	$\sigma / \text{Å}$	$\epsilon / \text{kcal mol}^{-1}$	q / e
NMP	C1	3.500	0.066	0.020
	C2	3.500	0.066	-0.120
	C3	3.500	0.066	-0.180
	HA	0.000	0.000	0.300
	N	3.250	0.170	-0.500
	C	3.750	0.105	0.500
	O	2.960	0.210	-0.500
	H11	2.500	0.030	0.060
	H12	2.500	0.030	0.060
	H13	2.500	0.030	0.060

(Cont.)

H21	2.500	0.030	0.060
H22	2.500	0.030	0.060
H31	2.500	0.030	0.060
H32	2.500	0.030	0.060
H33	2.500	0.030	0.060

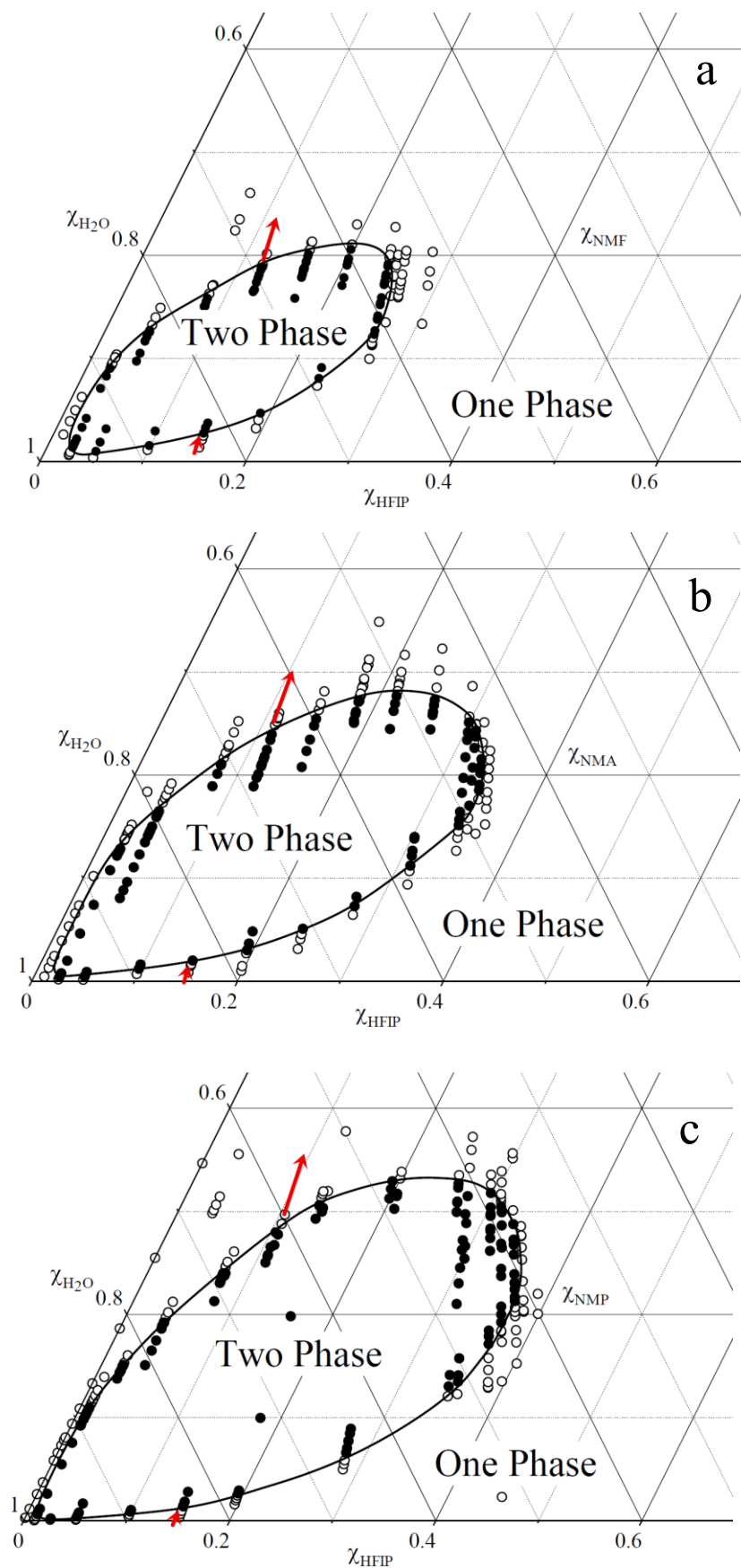


Fig. S2 Phase diagrams of amide–HFIP–water ternary systems at 298.2 ± 0.3 K as a function of mole fractions of amide, x_A , HFIP, x_{HFIP} , and water, $x_{\text{H}_2\text{O}}$: (a) NMF, (b) NMA, and (c) NMP systems. Compositions of the systems examined are indicated by opened circles (miscible) and filled ones (immiscible). The solid line gives the border between one-phase and two-phase states. The red arrows indicate the variation in the compositions of sample solutions examined by SANS, NMR, and MD.

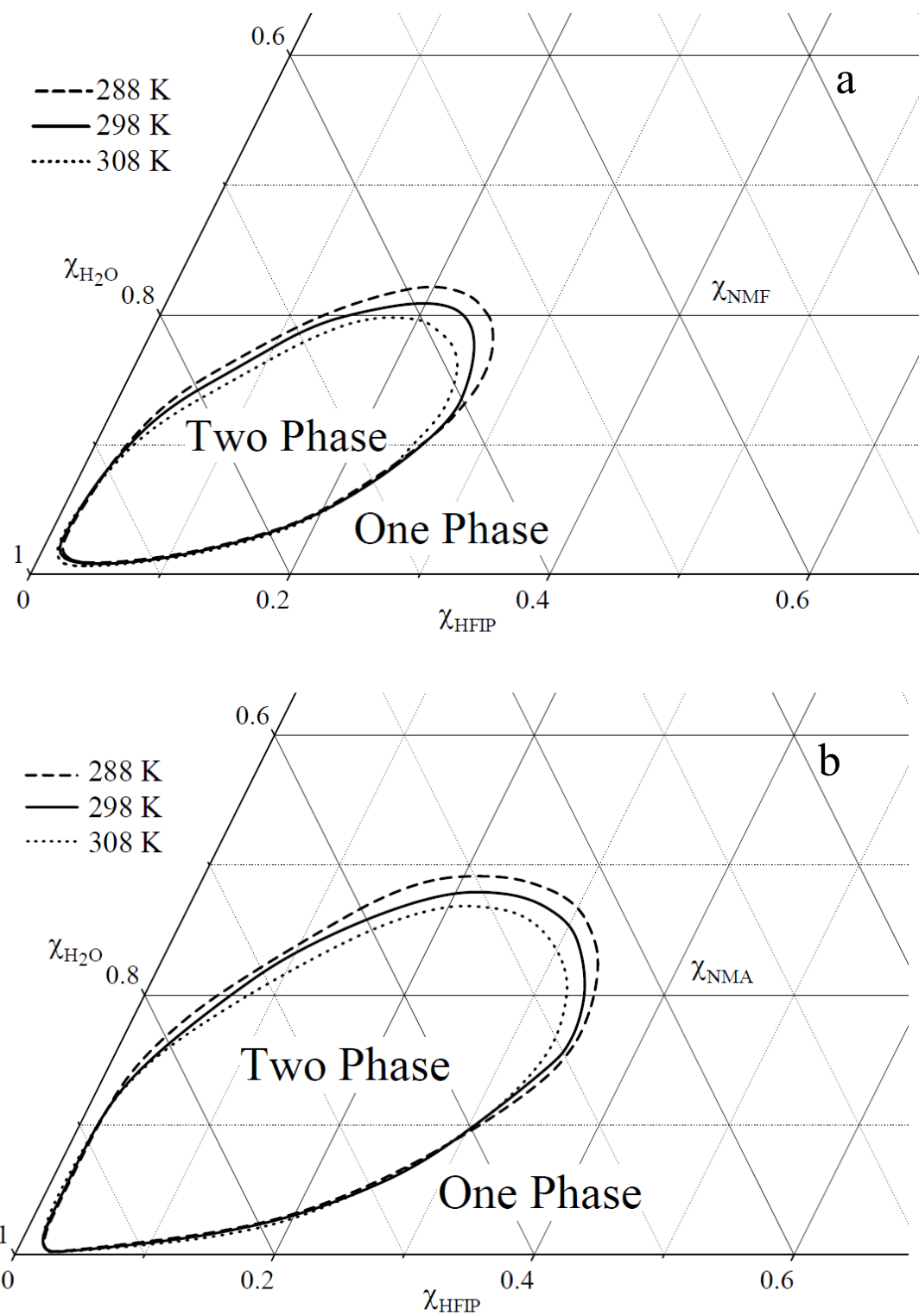


Fig. S3 Temperature dependence of phase diagrams of (a) NMF-HFIP-H₂O and (b) NMA-HFIP-H₂O systems.

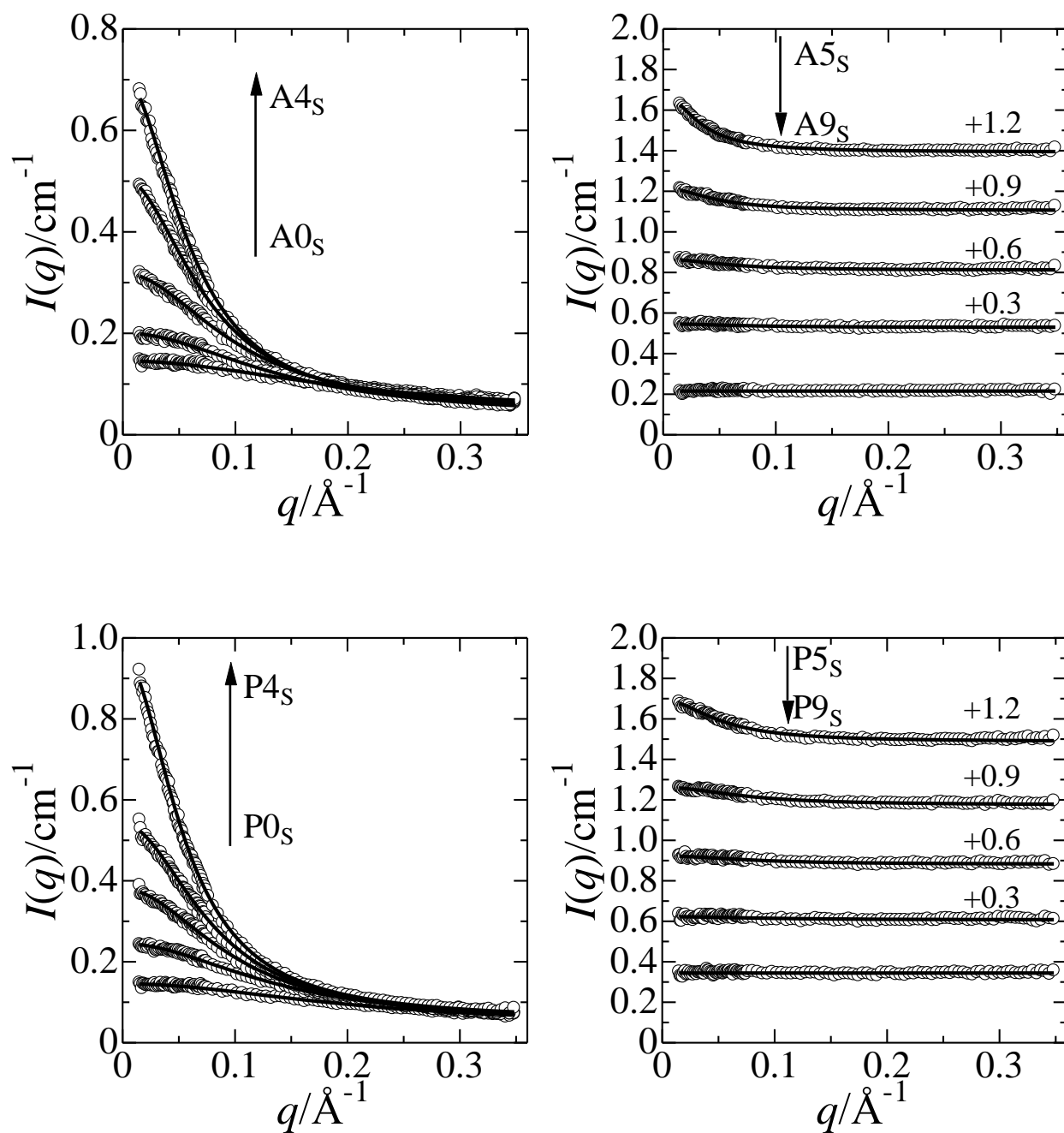


Fig. S4 SANS intensities of NMA-HFIP-D₂O (upper) and NMP-HFIP-D₂O (lower) mixtures: the left panels show the intensities of the mixtures below the $x_{A,298}^L$, and the right ones indicate those above the $x_{A,298}^U$. The circles are the observed values and the solid lines are the theoretical ones obtained from the Ornstein-Zernike fits using a least-squares refinement procedure. The values in the right panels indicate the intensities shifted from the origin to avoid overlap of the plots. The arrows show the increase in the amide concentration.

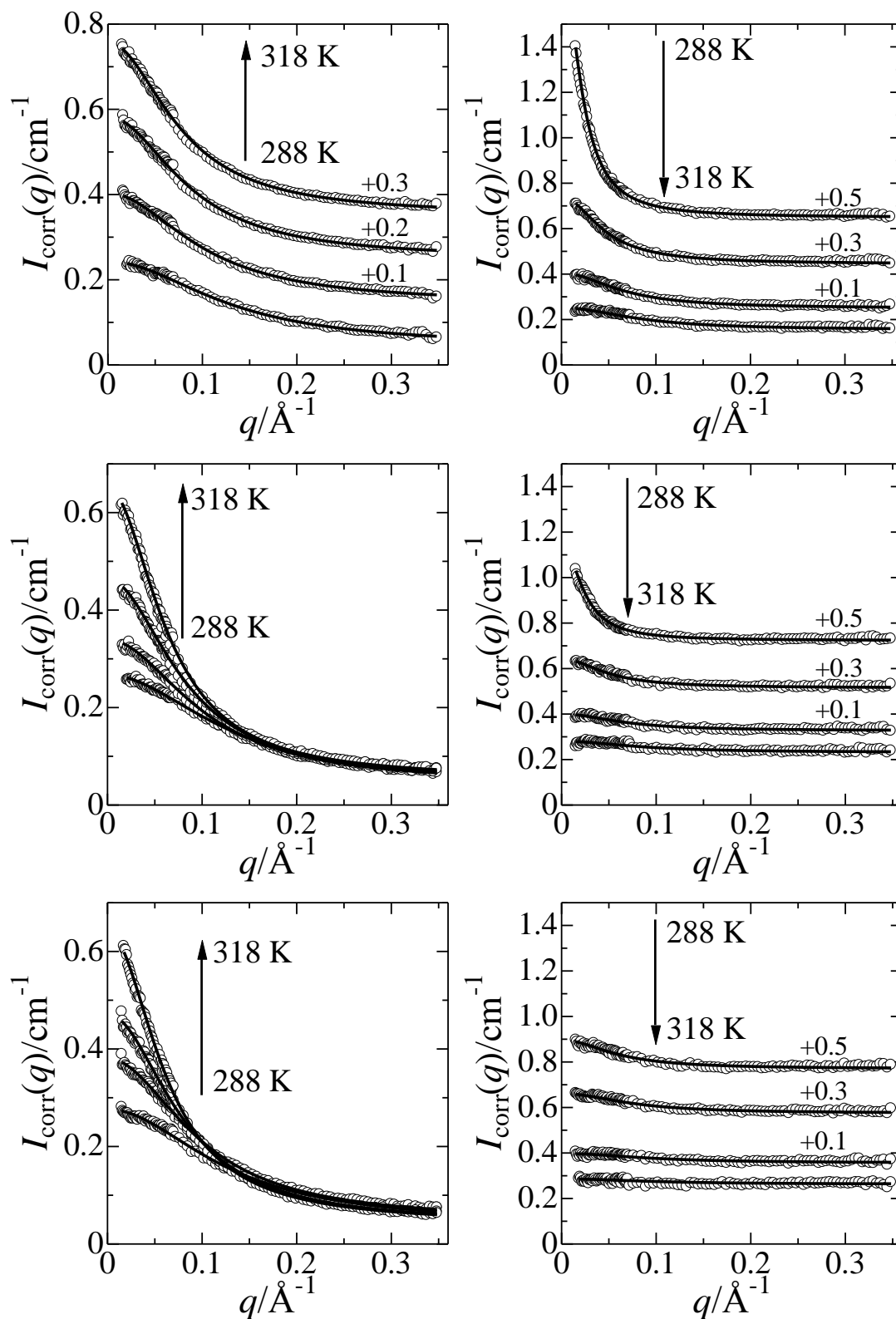


Fig. S6 SANS intensities of amide–HFIP–D₂O mixtures (NMF: upper; NMA: middle; NMP: bottom) as a function of temperature. The left and right panels show the intensities of the NMF systems of F2_S and F6_S, the NMA ones of A2_S and A6_S, and the NMP ones of P2_S and P6_S, respectively. The circles are the observed values, and the solid lines are the theoretical ones obtained from the Ornstein–Zernike fits using a least-squares refinement procedure. The values in the figures indicate the intensities shifted from the origin to avoid overlap of the plots. The arrows show the rise in temperature.

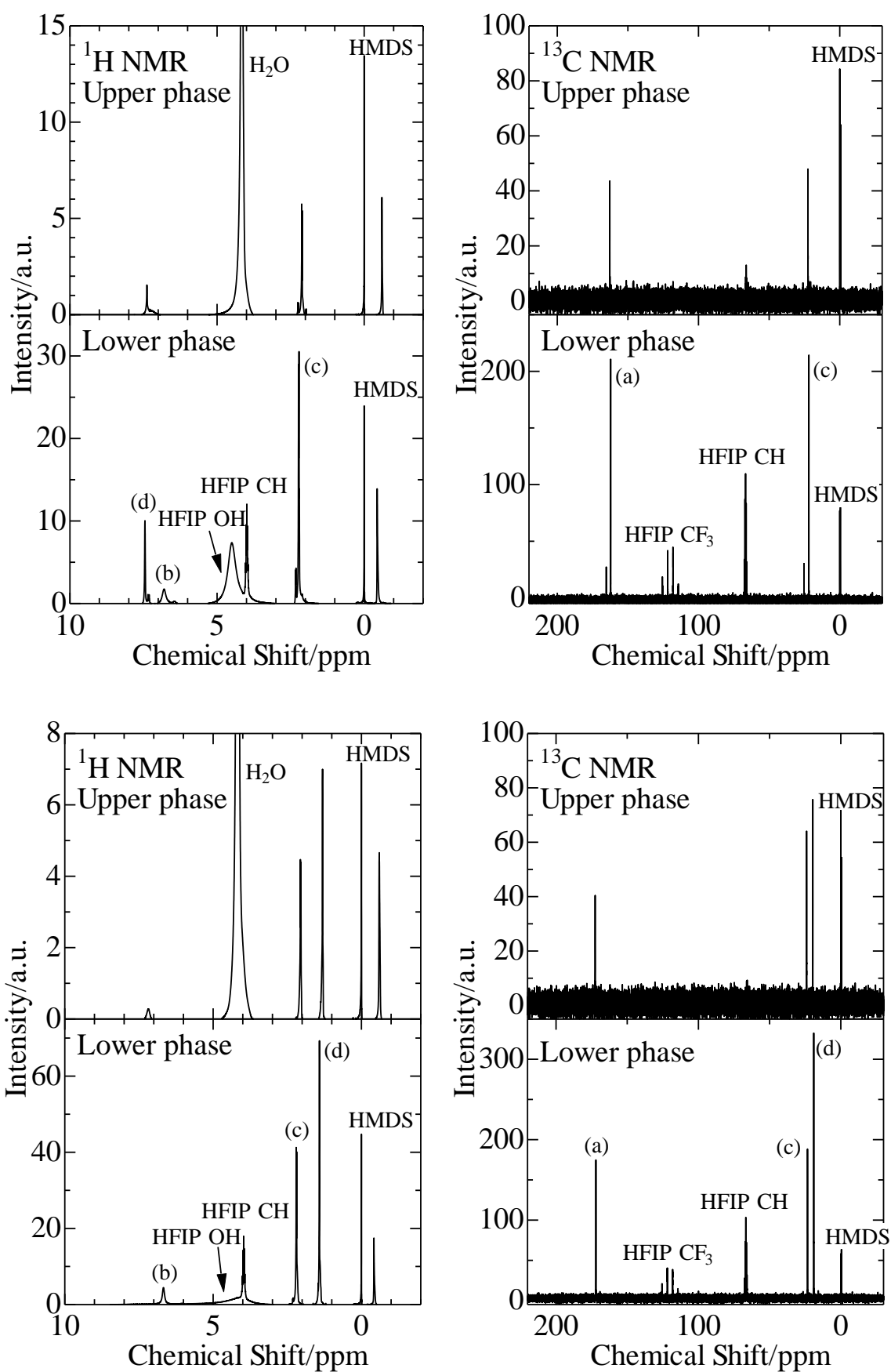


Fig. S7 ^1H and ^{13}C NMR spectra of upper and lower phases separated from NMF-HFIP-H₂O (upper) and NMA-HFIP-H₂O (lower) systems at 298 K.

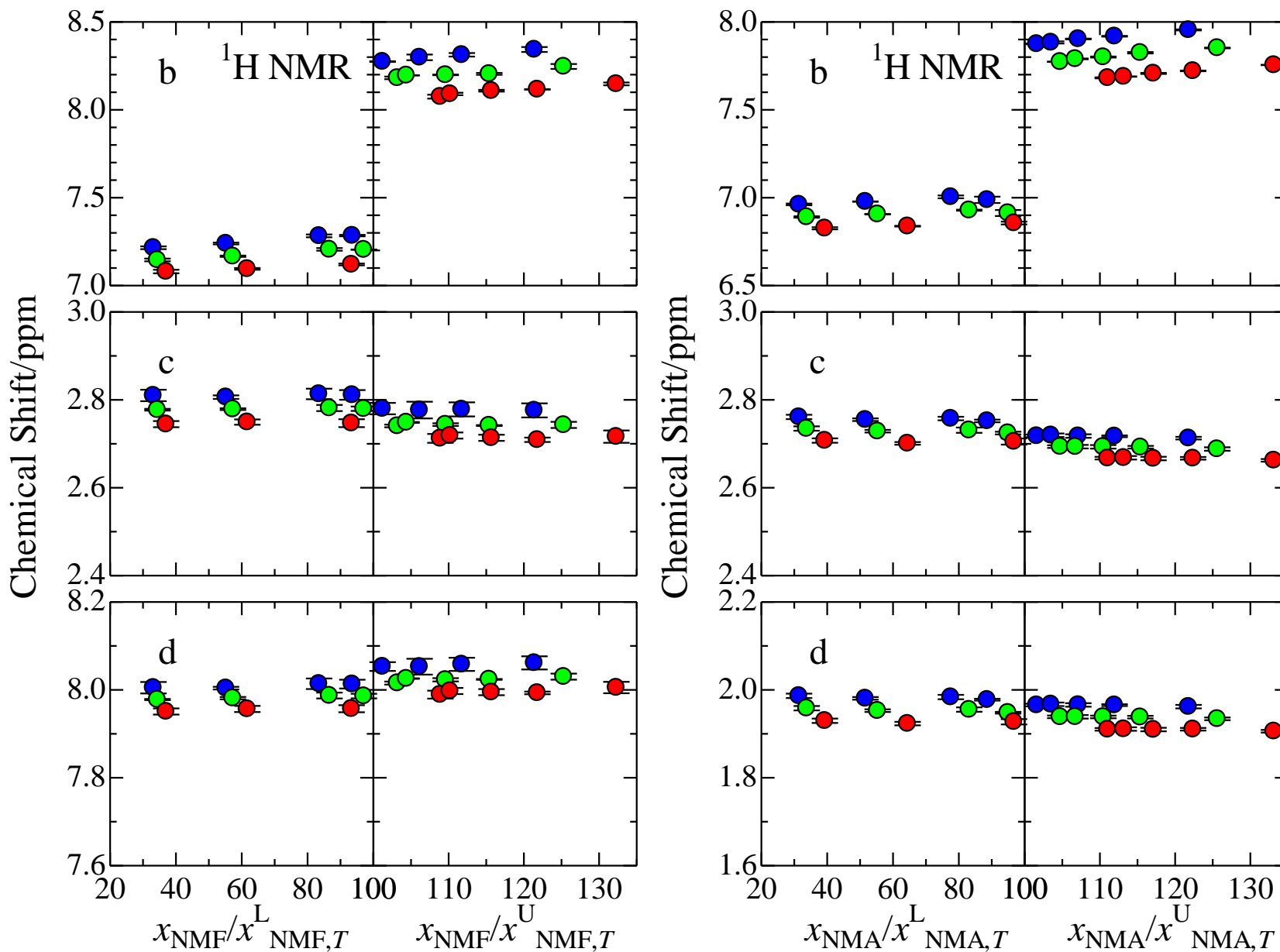


Fig. S8 ^1H chemical shifts of amide molecules in NMF-HFIP-H₂O (left, F_{1N}-F_{4N} and F_{5N}-F_{9N}) and NMA-HFIP-H₂O (right, A_{1N}-A_{4N} and A_{5N}-A_{9N}) mixtures at 288 (blue circles), 298 (green ones), and 308 K (red ones) as a function of the ratio of amide mole fraction to the phase separation one at each temperature. The standard deviations are shown by error bars.

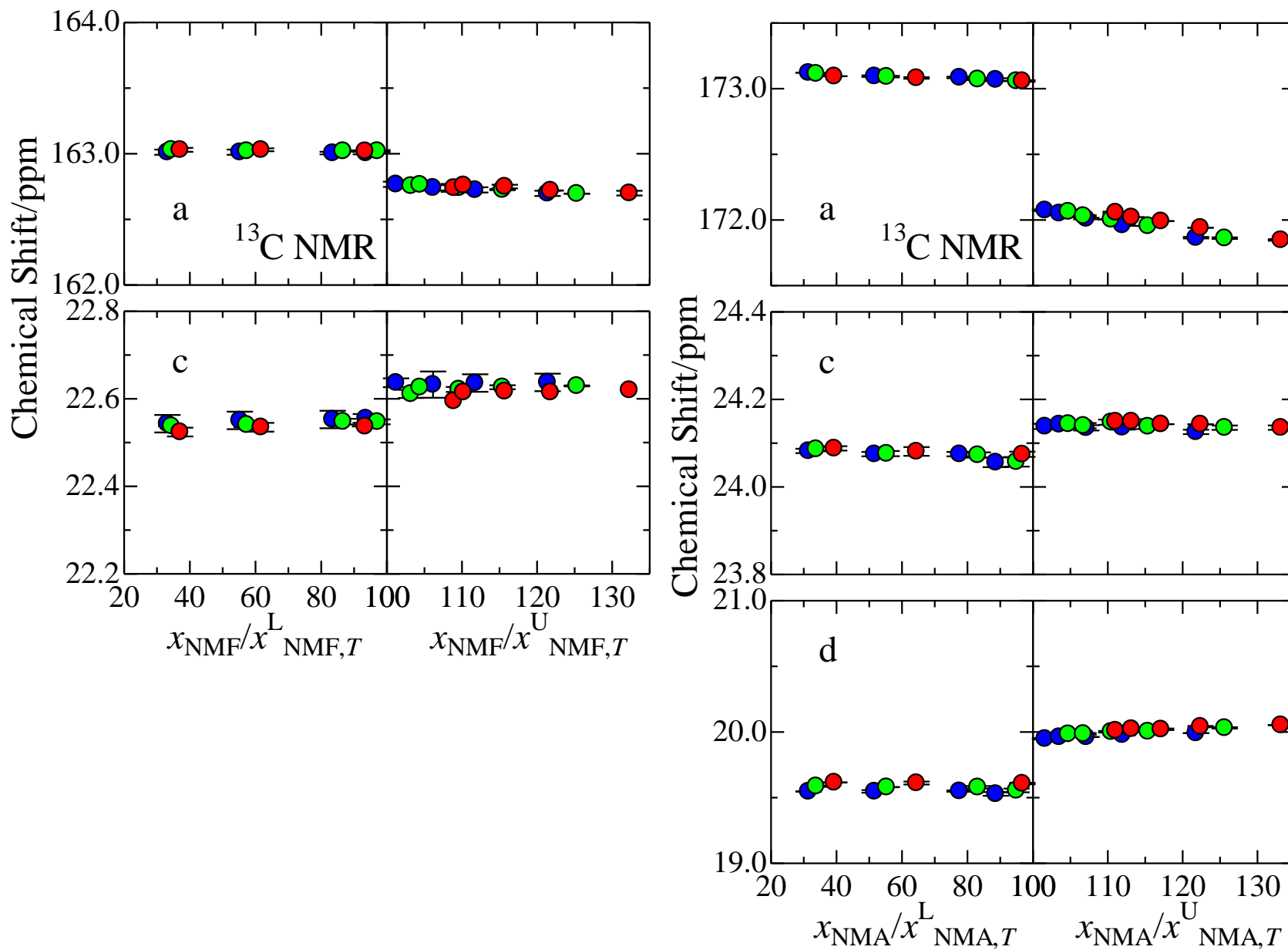


Fig. S9 ^{13}C chemical shifts of amide molecules in NMF-HFIP-H₂O (left, F1_N-F4_N and F5_N-F9_N) and NMA-HFIP-H₂O (right, A1_N-A4_N and A5_N-A9_N) mixtures at 288 (blue circles), 298 (green ones), and 308 K (red ones) as a function of the ratio of amide mole fraction to the phase separation one at each temperature. The standard deviations are shown by error bars.

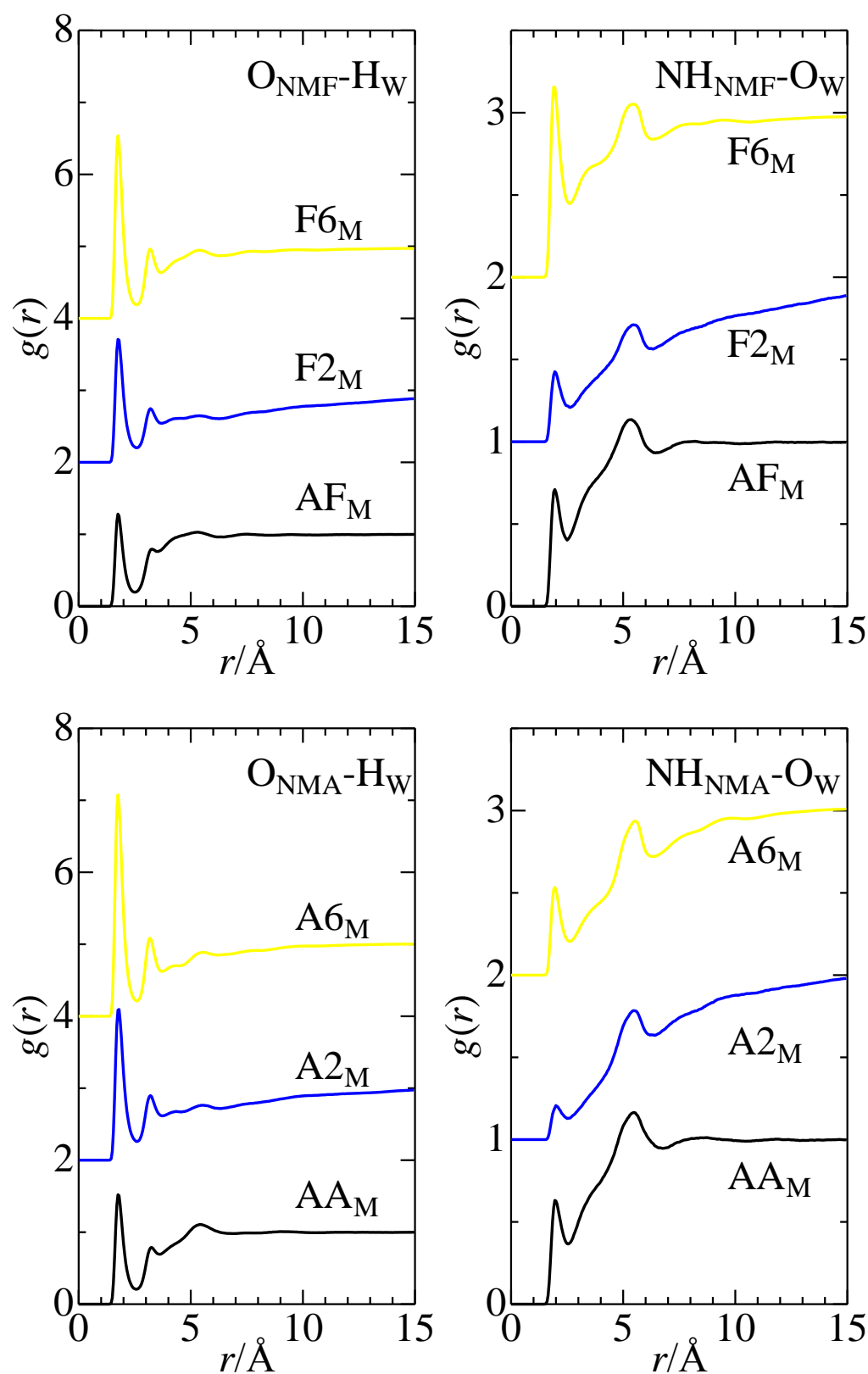


Fig. S10 Intermolecular atom-atom pair correlation functions $g(r)$ for $O_A-\text{H}_W$ interaction between the amide carbonyl oxygen and water hydroxyl hydrogen atoms (left) and NH_A-O_W interaction between the amide amino hydrogen and water oxygen atoms (right) obtained from MD simulations on amide-water systems (black line), amide-HFIP-water systems below the $x_{A,298}^L$ (blue one) and above the $x_{A,298}^U$ (yellow one). The upper and lower panels show the $g(r)$ of the NMF and NMA systems, respectively.

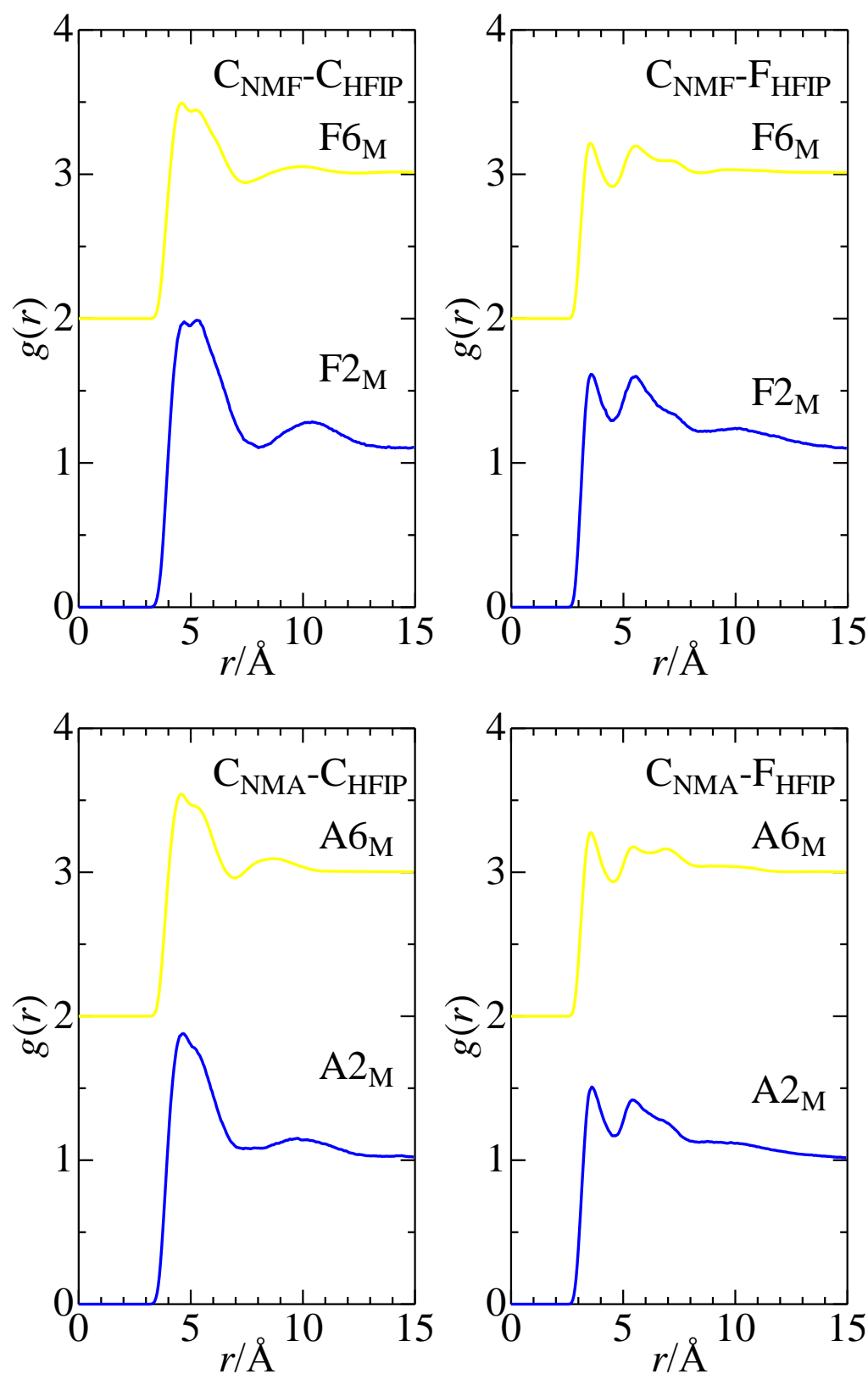


Fig. S12 Intermolecular atom-atom pair correlation functions $g(r)$ for $C_{\text{A}}-C_{\text{HFIP}}$ interaction between the amide carbon and HFIP carbon atoms and $C_{\text{A}}-F_{\text{HFIP}}$ interaction between the amide carbon and HFIP fluorine atoms obtained from MD simulations on amide-HFIP-water systems. The colors of lines are the same as those used in Fig. S10. The upper and lower panels show the $g(r)$ of the NMF and NMA systems, respectively.

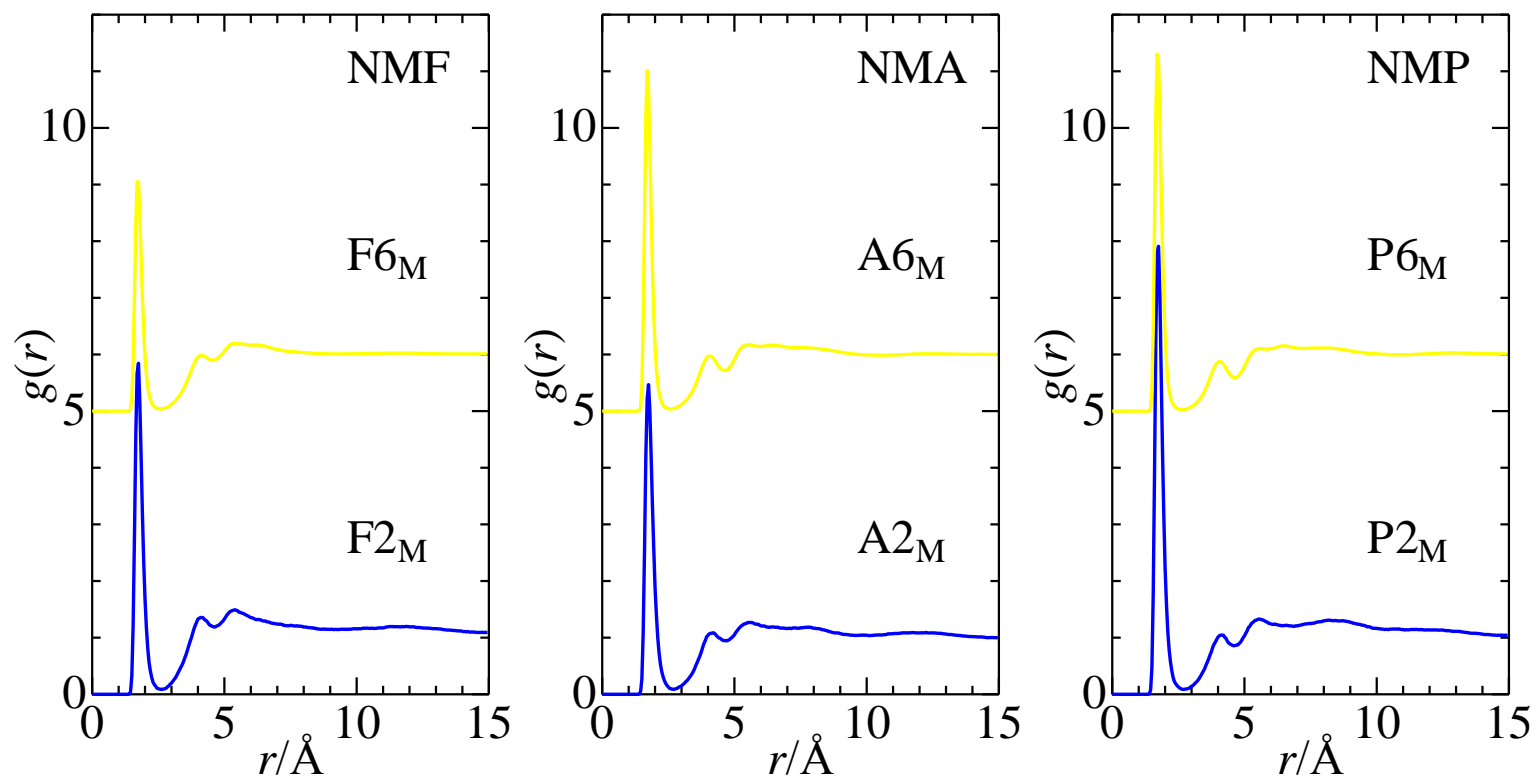


Fig. S13 Intermolecular atom–atom pair correlation functions $g(r)$ for O_A-H_{HFIP} interaction between the amide carbonyl oxygen and HFIP hydroxyl hydrogen atoms obtained from MD simulations on amide–HFIP–water mixtures below the $x_{A,298}^L$ (blue) and above the $x_{A,298}^U$ (yellow). The left, center, and right panels show the $g(r)$ of the NMF, NMA, and NMP systems, respectively.

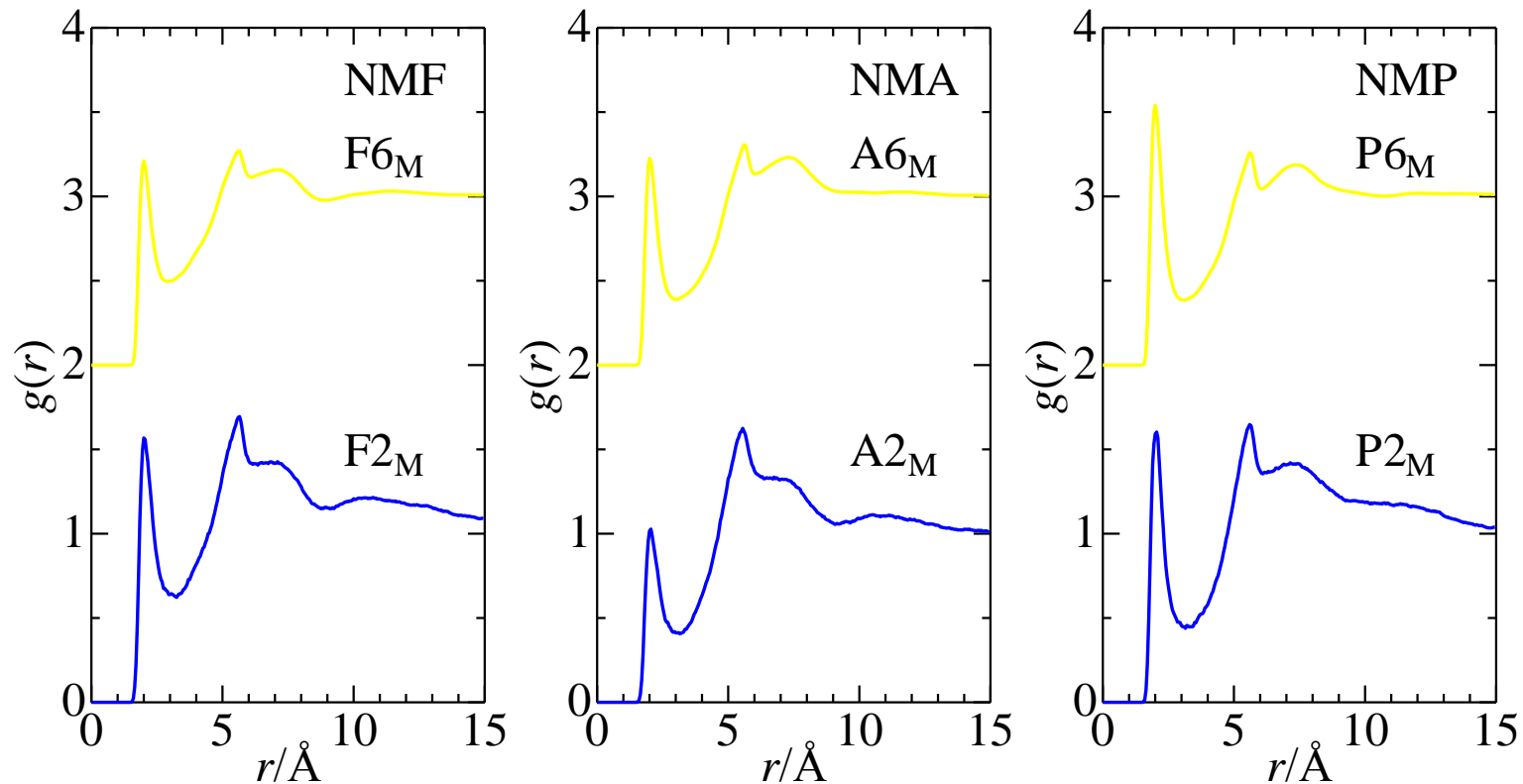


Fig. S14 Intermolecular atom-atom pair correlation functions $g(r)$ for $\text{NH}_A\text{-O}_{\text{HFIP}}$ interaction between the amide amino hydrogen and HFIP hydroxyl oxygen atoms obtained from MD simulations on amide-HFIP-water mixtures below the $x_{A,298}^L$ (blue) and above the $x_{A,298}^U$ (yellow). The left, center, and right panels show the $g(r)$ of the NMF, NMA, and NMP systems, respectively.

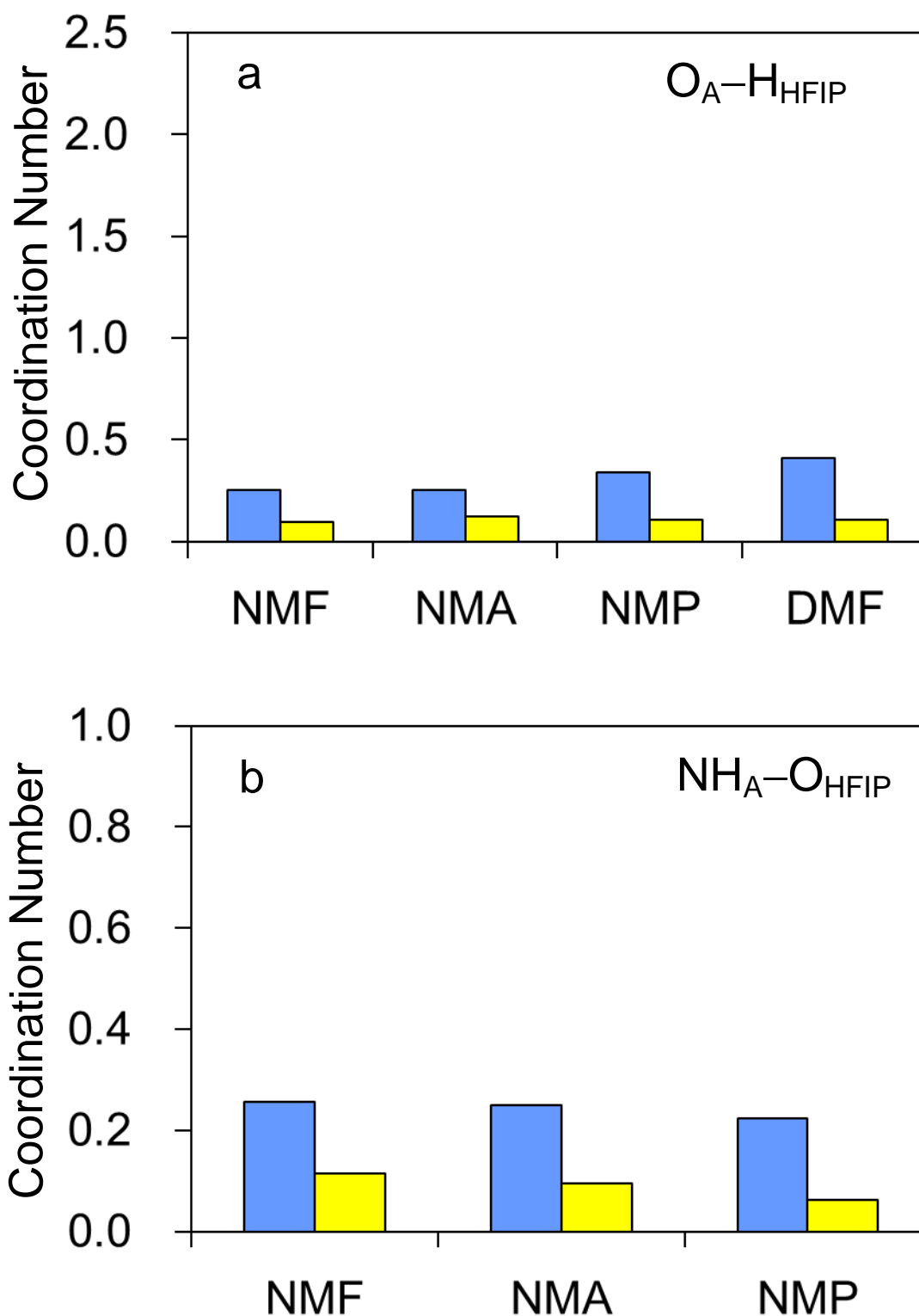


Fig. S15 Numbers of hydrogen bonds for (a) O_A-H_{HFIP} and (b) NH_A-O_{HFIP} estimated from MD $g(r)$. The blue and yellow columns represent those for amide-HFIP-water systems below the $x_{A,298}^L$ and above the $x_{A,298}^U$, respectively.